

THE RHIC LATTICE*

S.Y. Lee, J. Claus, E.D. Courant, H. Hahn and G. Parzen
Brookhaven National Laboratory
Upton, N.Y. 11973

Abstract

An antisymmetric lattice for the proposed Relativistic Heavy Ion Collider at Brookhaven National Laboratory is presented, which has been designed to have (1) an energy range from 7 GeV/amu up to 100 GeV/amu; (2) a good tunability of β^* and betatron tune; (3) freedom in the choice of crossing angle between beams; and (4) capability of operating unequal species, for example, proton on gold. Suppression of structure resonances is achieved by a proper choice of the phase advances across the insertion and the arc cells.

Introduction

Recent progress in theoretical and experimental discoveries in nuclear and particle physics points to the importance of physics made available by heavy ion collisions.¹⁻² A dedicated Relativistic Heavy Ion Collider (RHIC) is being studied at this Laboratory.³

The design for RHIC satisfies a number of requirements: (1) covering the energy from 7 GeV/amu up to 100 GeV/amu, (2) a luminosity of 10^{25} - 10^{27} /cm²sec for heavy ions such as gold on gold and luminosity of 10^{31} - 10^{32} /cm²sec for proton on proton, (3) a ± 10 m free space in the crossing region for experimental equipment, (4) operation of unequal species such as proton on gold, (5) operating different crossing angles within ± 2 mrad, and (6) capacity for changing β^* independently at each crossing point. Most importantly, the accelerator has to fit into the existing CBA tunnel.

Heavy ions are characterized by small values of q/A and large ones for q^2/A , where q and A are charge and mass numbers of ions. The large intrabeam Coulomb scattering, due to large q^2/A , demands stronger focusing for the beam particles. Therefore the transition energy of the machine is correspondingly high ($\gamma_t = 25 \sim 35$). The injection energy is determined by the maximum $B\rho$ value available in the AGS, where $B\rho \approx 100$ Tm or $\gamma_{inj} \approx 12$ for Gold beam. Acceleration through the transition energy is clearly unavoidable for heavy ions. On the other hand, since Landau damping becomes ineffective at the transition energy, it appears preferable to have a low transition energy γ_t to control the total growth of the longitudinal phase space area.⁶ Careful studies including all the other aspects such as rate of acceleration, r.f. parameters, aperture of magnets have been performed to choose an appropriate γ_t and tune. From these studies, it appears that the longitudinal momentum amplitude of the bunched beam at the transition is about $\Delta p/p \approx 1\%$. Thus an accelerator with good chromatic properties is important.⁷

In this paper, we present a lattice which satisfies these constraints. We discuss the ring structure, the regular cells in the arc, the insertion layout and the betatron amplitude functions, and the stopband bandwidth of the structure resonances and method of minimizing the effects of these stopbands.

RHIC Ring Structure

Each of the two rings of RHIC is composed of six arcs and six insertions interconnecting these arcs. Each arc consists of 12 FODO cells and each in-

sertion has nine quadrupoles and four dipoles (two for dispersion suppressor and two for beam crossing) on each side of the crossing point. Figure 1 shows the global structure of the collider rings, where A_I and A_O stand for inner and outer arcs and C_{IO} and C_{OI} for insertions from inner arc to outer arc and from outer arc to inner arc respectively. The polarity sequence of all quadrupoles is anti-symmetric with respect to all crossing points. However the sequence is symmetric with respect to the arc centers.

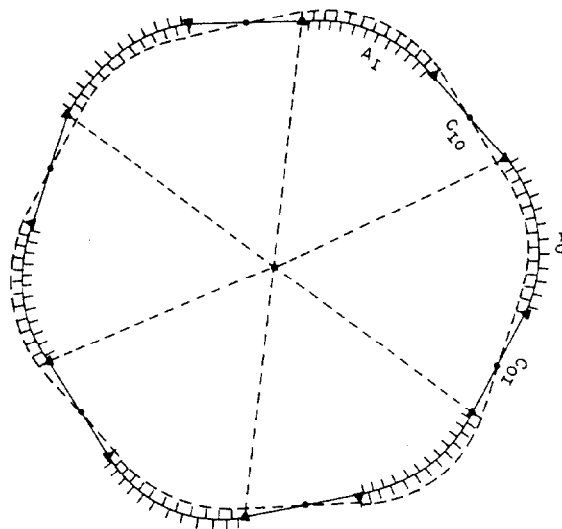


Fig. 1. Ring structure.

We have chosen $\pi/2$ phase advance for each FODO cell of length 29.6 m. This focusing strength is adequate for intrabeam Coulomb scattering consideration. At 90° phase advance in each cell with 12 cells per arc, the contribution of systematic chromatic structure resonance stopbands due to quadrupoles and sextupoles is minimized. The beam-beam separation between two rings in the arc is 60 cm for the convenience of magnet construction. Table 1 lists relevant parameters for these FODO cells.

Table 1. Principal Characteristics of Arc Cells

	Inner Arc	Outer Arc
Length (m)	29.5988	29.6454
Deflection Angle (mrad)		77.7007
Average radius of curvature (m)	380.9335	381.5332
Distance between centerlines (m)		.6
Dipole strength $\int B ds / B\rho$.03885
Quadrupole strength $\int B' ds / B\rho$ (m ⁻¹) F/D		.1007/.1000
Betatron phase adv. $\Delta\psi_H/2\pi$ $\Delta\psi_V/2\pi$.25 \pm .005
$\hat{\beta}_H, V/\hat{\beta}_H, V$ in quad. midplanes (m)	49.86/8.64	49.97/8.6
$\hat{\chi}_p/X_p$ in quad. midplanes (m)		1.53/.74

*Work performed under the auspices of the U.S. Department of Energy.

Insertions

The geometry of the insertion is composed of (1) a dispersion matching section (Q9, Q8, Q7, BS2, Q5, BS1 and Q5), (2) a straight betatron function matching section of a doublet quadrupole lenses Q5, and Q4 and a triplet lenses Q3, Q2 and Q1; and (3) the beam crossing dipoles BC2 and BC1. Figure 2 shows the detailed geometry of the insertion on one side of the crossing point (CR). The other half of the insertion is mirror symmetric in magnet distribution. BS1 of the inner and outer insertions serve also to bring the beam-beam separation to 35 cm at the edge of BC2. The magnets Q3, Q2, Q1 and BC2 of inner and outer insertions sit in the common vacuum vessels (dual magnets). All magnets in the insertions except BS1 and BS2 are separately adjustable. BC1 is common to both beams. Figure 3 shows the detailed BC1 and BC2 configuration. For equal species, the maximum crossing angle is 7 mrad due to the aperture limitation of BC1 (20 cm coil i.d.). The collision of unequal species is obtained by exciting BC2 in each of two rings separately with a common field of BC1.⁸ Figure 4 shows the betatron and dispersion functions in the insertion region respectively.

β^* can be adjusted in the range $3\text{ m} < \beta^* < 10\text{ m}$ by changing the gradients of the insertion quadrupoles without changing the transfer matrix across the insertion. This has been demonstrated in a smooth continuous fashion. Figure 5 shows the maximum β function, $\hat{\beta}$, and the natural chromaticity, χ_N , in the insertion as a function of β^* . The six arcs contribute -24 units of natural chromaticity. The contributions from six insertions varies from -16 to -33 for β^* from 10 m to 3 m.

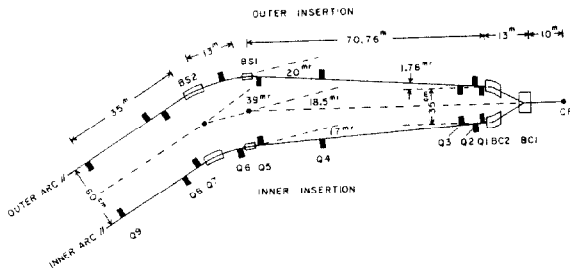


Fig. 2. Insertion layout.

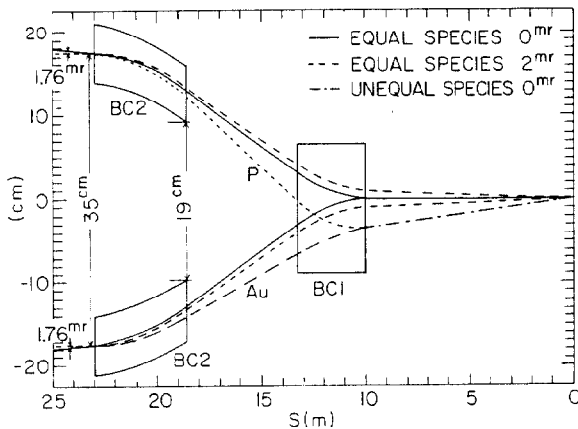


Fig. 3. Beams crossing geometry.

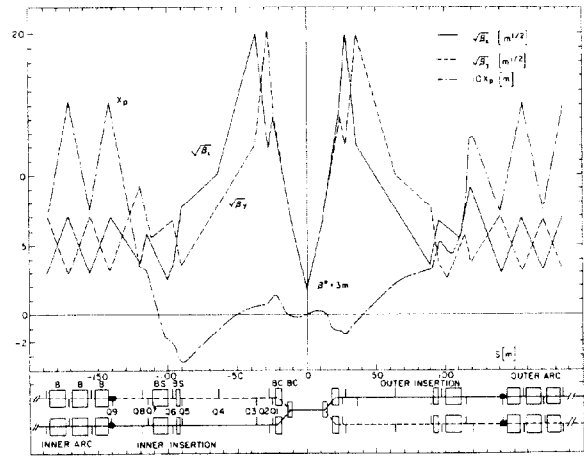


Fig. 4. Betatron and dispersion function.

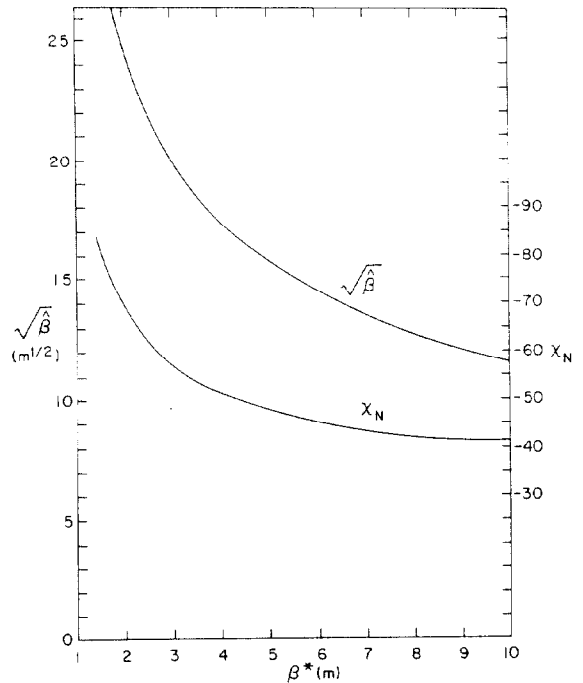


Fig. 5. Maximum $\hat{\beta}$ and natural chromaticity χ_N vs β^* .

Structure Resonances

The stopband width for the half-integer structure resonances of off-momentum particles is given by

$$\Delta\nu_{2n} = \frac{1}{2\pi} \frac{\Delta p}{p} \left| \int \beta(\kappa - \kappa') \chi_p e^{-i2n\psi} ds \right| = \frac{|J_{2n}|}{2\pi} \frac{\Delta p}{p} \quad (1)$$

where $\kappa = B'/B\rho$, $\kappa' = B''/B\rho$, β and χ_p are the beta and dispersion functions, and $\psi = \nu^{-1} \int ds/\beta$ is the betatron phase. The integral J_{2n} can be decomposed into contributions of arcs, A_I and A_0 , and insertions, C_{I0} and C_{O1} , respectively i.e.

$$J_{2n} = 3 (J_{2n}(A_I) - J_{2n}(A_0) + J_{2n}(C_{I0}) - J_{2n}(C_{O1})) \quad (2)$$

at $2n = 57, 63, 69$ etc. The factor 3 stems from the superperiodicity of the machine.

For a machine with six-fold superperiodicity, one has $J_{2n}(A_I) = J_{2n}(A_0)$ and $J_{2n}(C_{I0}) = J_{2n}(C_{O1})$. The corresponding half integer stopband width would be zero at $\nu = 28.5, 31.5$ and 34.5 respectively.

For a machine with three-fold superperiodicity, we have to choose phase advance in each arc cell such that

and $J_{2n}(A_I) \approx J_{2n}(A_0) \approx 0$ (3a)

$J_{2n}(C_{IO}) - J_{2n}(C_{OI}) \approx 0$ (3b)

are satisfied respectively. Equation (3a) is achieved if the phase advance per cell is 60° or 90° for 12 cells per arc. Since the insertions C_{OI} and C_{IO} are mirror symmetric to each other with respect to the center of the arcs, we have

$$J_{2n}(C_{OI}) = e^{-i4\mu_I\pi} J_{2n}^*(C_{IO}), \quad (4)$$

where μ_I is the phase advance of each insertion. Therefore, condition (3b) becomes

$$J_{2n}(C_{IO}) - J_{2n}(C_{OI}) = J_{2n}(C_{IO}) - e^{-i4\mu_I\pi} J_{2n}^*(C_{IO}) \quad (5)$$

$$= J_{2n}(C_{IO}) (1 - e^{-i4\mu_I\pi} e^{+2i\phi})$$

where

$$\phi = \frac{1}{2} \arg \frac{J_{2n}^*(C_{IO})}{J_{2n}(C_{IO})} \quad (6)$$

Thus a proper choice of μ_I , i.e.

$$2\mu_I\pi - \phi = m\pi \quad m = 0, 1, 2, \dots, \quad (7)$$

leads to cancellation of the half integer stopband for neighboring insertions. In the practical application, the integral $J_{2n}(C_{IO})$ is dominated by a single quadrupole Q_{20} . The contribution to this integral due to the elements Q_{1I} , Q_{2I} , Q_{3I} tend to cancel each other due to the small phase advance across these elements. Therefore $\phi \approx 4\mu_{Q_{20}}\pi$. Thus Eq. (7) becomes

$$2\mu_I - 4\mu_{Q_{20}} = 4(\mu_I - \mu_{Q_{20}}) - 2\mu_I = \text{integer} \quad (8)$$

This condition (Eq. (8)) is approximately satisfied in the RHIC design.

The third integer structure resonance can also be minimized by the choice of 90° phase advance per cell, where 12 cells per arc give local cancellation for these resonances. Since a variation of the machine betatron tune is obtained by changing the phase

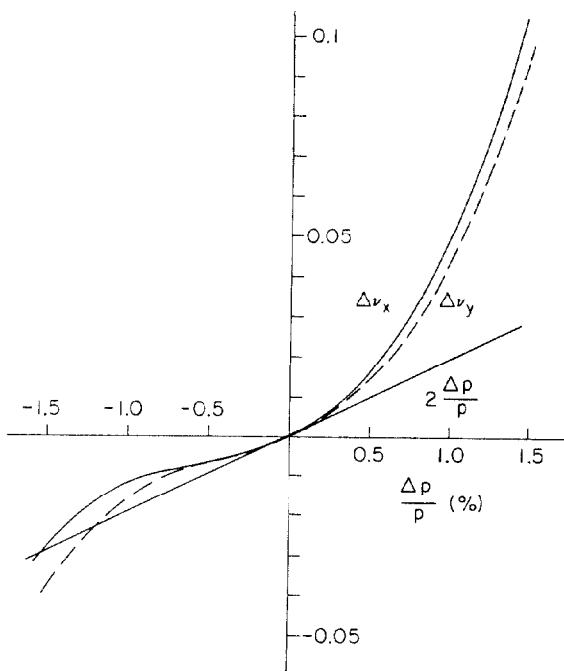


Fig. 6. ν vs $\Delta p/p$.

advances per cell, we cannot expect complete cancellation of the third integer structure resonance. The full stopband width is calculated to be .008 at $\nu = 28$ and .044 at $\nu = 29$, for 2 families of sextupoles in the chromaticity correction.

At $\beta^* = 3$ m, the natural chromaticity χ_N is about -57. Two families of sextupoles are used to correct the natural chromaticity to +2. Figure 6 shows the tune modulation for the off-momentum particles. We observe that at $\Delta p/p = +1\%$, the nonlinear part contributes .03 to the tune shift. Figure 7 shows the amplitude function modulation and momentum function modulation respectively. These modulations can be further reduced by increasing the number of sextupole families.

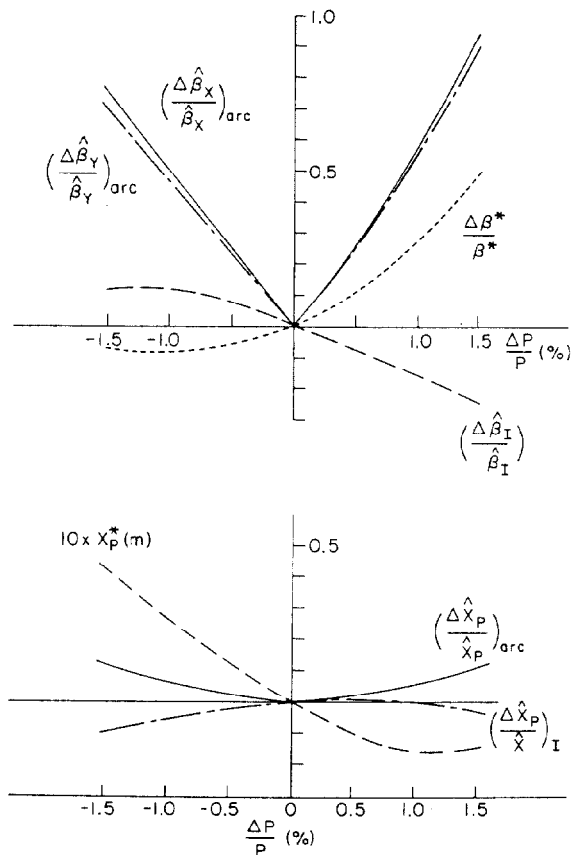


Fig. 7. β and X_p vs $\Delta p/p$.

References

1. G. Baym, "Major Facilities for Nuclear Physics," Physics Today, Vol. 38, p. 40, March 1985.
2. "Proc. Third Int. Conf. on Ultra-Relativistic Nucleus-Nucleus Collisions," T. Ludlam, H. Wegner, eds., Nucl. Phys. A418 (1984).
3. "RHIC and Quark Matter," BNL 51801
4. A. Pinwinsky, Proc. 9th Int. Conf. on High Energy Accelerators, p. 405 (1974); J.D. Bjorken and S.K. Mtingwa, Particle Accelerators, Vol. 13, p. 115 (1983).
5. G. Parzen, "Strong Intrabeam Scattering in Proton and Heavy Ion Beams," these proceedings.
6. S.Y. Lee and J.M. Wang, "Microwave Instability Across the Transition Energy," these proceedings.
7. J. Claus, M. Cornacchia, E.D. Courant, G.F. Dell, G. Parzen and A. Garren, IEEE Transactions on Nucl. Science, NS-30, 2451 (1983).
8. M. Barton and R. Palmer, private communications.